PDL Localization and Estimation through Linear Least Squares-based Longitudinal Power Monitoring

Lorenzo Andrenacci, Gabriella Bosco and Dario Pilori

***Abstract*—A novel algorithm capable of localizing Polarization-Dependent Loss (PDL) and directly estimating its value in a multi-span optical transmission link using only Rx-side Digital Signal Processing (DSP) is proposed. The algorithm employs a Linear Least Squares-based power profile estimation method and it succeeds in localizing multiple PDL sources along the link. Its performance is evaluated across diverse power levels, including SNR-maximizing ones, resulting in consistently comparable results.**

I. Introduction

THE accurate monitoring of optical links plays a critical role in the operation and management of an optical network. Traditionally, Optical Time-Domain Reflectometers (OTDRs) have been employed within the network for this purpose. However, the accurate monitoring of an entire link may require several OTDRs, which can become prohibitively expensive for large optical networks. Recently proposed alternatives are based on Longitudinal Power Monitoring (LPM) algorithms [1]–[5], which exploit the digital data available inside the standard coherent receivers, eliminating the need for external hardware (e.g., OTDRs). This approach offers a cost-effective solution for monitoring the optical link. Two primary families of methods were proposed to achieve LPM: correlation-based [1]–[3] and Least Squares (LS)-based methods [6].

Traditionally, LPM has primarily been employed for power profile estimation. However, recent research has explored its potential for estimating additional parameters, broadening its applicability in optical network analysis. For instance, some works have successfully estimated chromatic dispersion [6], Multi-Path Interference (MPI) [3], and Polarization-Dependent Loss (PDL) [7], [8] using LPM techniques. In particular, PDL can introduce a significant penalty on the link performance, and its effects are closely tied to the specific locations of PDL sources [9]. As a result, precise monitoring of the PDL source positions becomes crucial.

In [7], [10] a correlation-based LPM was used for PDL estimation. However, correlation-based LPM methods have several drawbacks [11], such as limited spatial resolution, modulation-format dependence and need for pre-calibration. Moreover, in [7], [10] the transmit power was significantly higher than the optimal (i.e. SNR-maximizing) values, and the link distance was shorter than the reach of the considered modulation formats. In [8], the PDL is estimated with a linear LS (LLS)-based approach. Compared to correlation-based LPM, the PDL is directly estimated from the power profiles, without pre-calibration, allowing for a lower computational complexity. However, in [8], the link had only a single PDL source, the transmit power was higher than optimal, and the length was shorter than the typical reach of the modulation format.

In this Letter, we apply a LLS-based approach to a 10×50 km SMF link with PM-64QAM with multiple PDL elements in the link. Compared to [8], we were able to correctly estimate the amount and position of the PDL elements also at lower, SNR-maximizing, power levels.

Manuscript received July 2023; revised September 2023.This work was partially supported by the European Union under the Italian National Recovery and Resilience Plan (NRRP) of NextGenerationEU, partnership on 'Telecommunications of the Future' (PE00000001 - program 'RESTART').

The authors are with the Department of Electronics and Telecommunications (DET), Politecnico di Torino, C.so Duca degli Abruzzi 24, 10129 Torino (TO), Italy. e-mail: lorenzo.andrenacci@polito.it.

II. PDL Estimation using eRP1-LLS

The technique introduced in [4], adopted in this work with suitable adjustments, provides a closed-form expression for estimating the longitudinal power profile of a polarization-multiplexed optical signal. The technique relies on the first-order enhanced Regular Perturbation (eRP1) model approximation [12], [13]. By leveraging this model, the original non-linear LS problem described in [6] is transformed into a LLS problem, for which an analytical solution exists.

In the coherent receiver, the transmitted signal $\mathbf{A}_{\mathrm{ref}}[0,n]$ is reconstructed and virtually propagated according to the eRP1 approximation, i.e., $\mathbf{A}_{\mathrm{ref}}[L,n] \simeq \mathbf{A}_{\mathrm{ref},0}[L,n] + \mathbf{A}_{\mathrm{ref},1}[L,n]$, where L is the length of the link and n is the discrete-time index. Specifically,

$$\mathbf{A}_{\mathrm{ref},0}[L,n] = D_{0,L}\left[\mathbf{A}_{\mathrm{ref}}[0,n]\right] \tag{1}$$

$$\mathbf{A}_{\mathrm{ref},1}[L,n] = \sum_{k=0}^{K-1} \gamma'_k g[z_k,n] \tag{2}$$

where

$$g[z_k,n] = -j\Delta z_k D_{z_k,L}\left[N_p\left[D_{0,z_k}\left[\mathbf{A}_{\mathrm{ref}}[0,n]\right]\right]\right] \tag{3}$$

$$\gamma'_k = \frac{8}{9}\gamma P(z_k) \tag{4}$$

In the above equations, $D_{z_i,z_j}[\cdot]$ is a linear operator which introduces chromatic dispersion (CD) from position z_i to z_j in the link; $N_p[\cdot] = \left(\|\cdot\|^2 - \frac{3}{2}P_A\right)(\cdot)$ is a non-linear operator, with P_A being the average power of $\mathbf{A}_{\mathrm{ref}}[z,n]$; γ is the non-linear coefficient of the fiber; $P(z_k)$ is the optical signal power, evaluated at position z_k, for $k \in [0,K]$; $\Delta z_k = z_{k+1} - z_k$ is the spatial step. The same approximation is applied to the received signal, i.e., $\mathbf{A}[L,n] \simeq \mathbf{A}_0[L,n] + \mathbf{A}_1[L,n]$. In particular, if the sampling rate satisfies the Nyquist criterion, the linear term can be expressed as $\mathbf{A}_0[L,n] \simeq \mathbf{A}_{\mathrm{ref},0}[L,n]$. As a result,

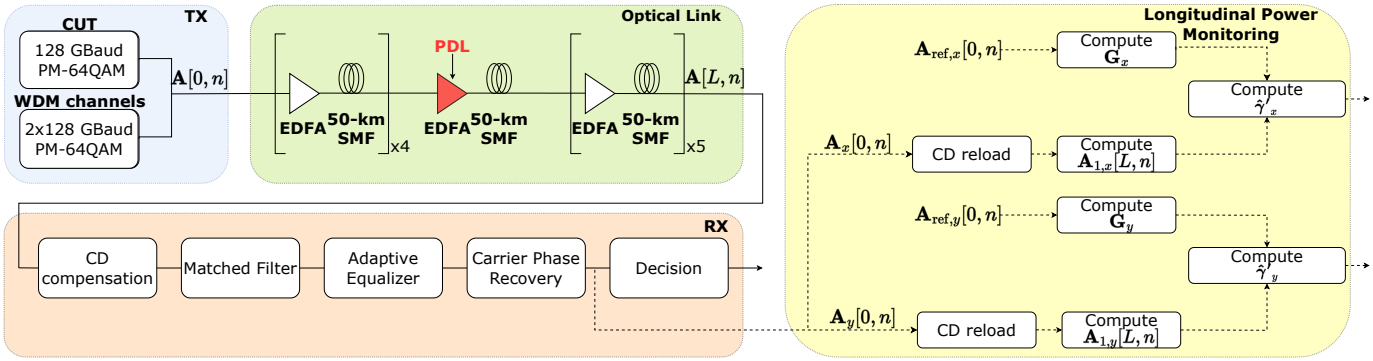

Fig. 1. Simulation setup (left) and longitudinal power monitoring algorithm schematic (right).

retrieving $\mathbf{A}_1[L,n]$ from $\mathbf{A}[L,n]$ and $\mathbf{A}_{\mathrm{ref},0}[L,n]$ becomes a straightforward process.

Assuming that P_A is normalized to 1, then the entire power profile evolution can be described by the vector $\boldsymbol{\gamma}' = \left[\gamma'_0, \ldots, \gamma'_{K-1}\right]^T$ [6]. The proposed linear least-squares solution [4] to estimate this profile is given by the equation:

$$\hat{\boldsymbol{\gamma}}' = \left(\mathrm{Re}\left[\mathbf{G}^\dagger \mathbf{G}\right]\right)^{-1} \mathrm{Re}\left[\mathbf{G}^\dagger \mathbf{A}_1[L,n]\right] \tag{5}$$

where $\mathbf{G}$ is a matrix defined as $(\mathbf{G})_{n,k} = g[z_k, n]$. The power profile along the fiber can then be computed as $P(z_k) = (9/8)\hat{\gamma}'_k/\gamma$. However, since PDL has a distinct impact on the two signal polarizations, a separate estimation of the power profile of each polarization is needed. To achieve this, similar to the approach employed in [10] for the correlation-based method, a separate vector $\hat{\boldsymbol{\gamma}}'_{x/y}$ is computed for each signal polarization, substituting the nonlinear operator $N_p[\cdot]$ with its single-polarization version in the eRP1 approximation, i.e., $N_{x/y}[\cdot] = \left(|\cdot|^2 - 2P_{x/y}\right)(\cdot)$.

III. Simulation Setup and Results

Fig. 1 shows a schematic of the simulation setup and of the LPM algorithm. The transmitted signal consists of three PM-64-QAM WDM channels having square-root raised-cosine spectral shape with roll-off 0.15, modulated at 128 GBaud and with a frequency spacing 200 GHz. The channel under test (CUT) is the central one. The link is composed of 10×50 km identical spans of SMF fiber, with attenuation $\alpha_{\mathrm{dB}} = 0.2\,\mathrm{dB/km}$, CD coefficient $\beta_2 = -21.28\,\mathrm{ps}^2/\mathrm{km}$ and nonlinearity coefficient $\gamma = 1.3\ 1/\mathrm{W/km}$. Each span is followed by an EDFA with noise figure 5 dB, working in constant output power mode to fully compensate for the span loss.

To evaluate the algorithm's performance, we conducted tests involving the insertion of lumped PDL elements into the optical link. In the Jones formalism, the effect of each PDL element on the optical signal $\mathbf{E}_{\mathrm{in}}$ can be represented by the following equation [10]:

$$\mathbf{E}_{\mathrm{out}} = \mathbf{R}^{-1} \begin{pmatrix} \sqrt{1+\epsilon} & 0 \\ 0 & \sqrt{1-\epsilon} \end{pmatrix} \mathbf{R}\mathbf{E}_{\mathrm{in}} \tag{6}$$

where $\mathbf{R}$ is a complex rotation matrix and ϵ is a parameter that represents the degree of PDL. The value of ϵ ranges from 0 to 1, and it indicates the amount of power imbalance between the two orthogonal polarizations. The PDL magnitude in logarithmic scale is given by $\mathrm{PDL_{dB}} = 10\log_{10}\left((1+\epsilon)/(1-\epsilon)\right)$.

In the simulations, fiber propagation is modeled using the split-step Fourier Method, which implements the Manakov equation [14]. After propagation, the optical signal enters a standard coherent receiver [15], where it undergoes sampling at a rate of 2 samples per symbol. Subsequently, the signal samples are processed by several DSP blocks, which perform CD compensation, matched filtering, LMS-based adaptive equalization and blind-phase search (BPS) carrier phase recovery. The output obtained from the last stage is then extracted and utilized as input for the LPM algorithm. In particular, each power profile is computed using approximately 8×10^5 samples, corresponding to the sample length of both $\mathbf{A}_1[L,n]$ and $\mathbf{G}$ in Eq. (5). Moreover, in the simulation we reconstruct exactly $\mathbf{A}_{\mathrm{ref}}[0,n]$ from the transmit sequence. In a realistic scenario, this reconstruction would typically occur after error-free Forward Error Correction (FEC) decoding, which was not implemented in this work.

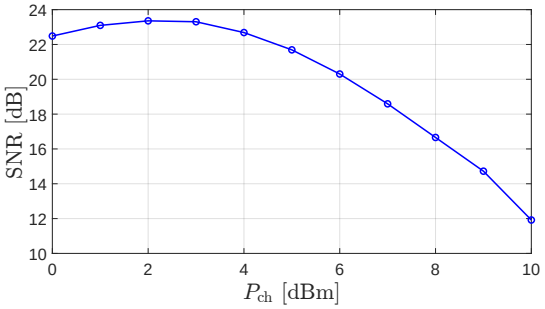

Fig. 2. Signal-to-Noise ratio (SNR) for different values of the transmitted power per channel P_{ch}.

Initially, we focused on estimating the location of a lumped 3-dB PDL element, inserted at the beginning of the 5th span, emulating a faulty wavelength-selective switch (WSS) placed after the EDFA. The estimation was performed at three different operating conditions. Firstly, the algorithm was tested at a high transmit power of 8 dBm, similarly to [7]. Subsequently, it was tested at lower power levels of 5 and 2 dBm, the latter corresponding to the launch power that maximizes the overall Signal-to-Noise Ratio (SNR), as shown in Fig. 2.

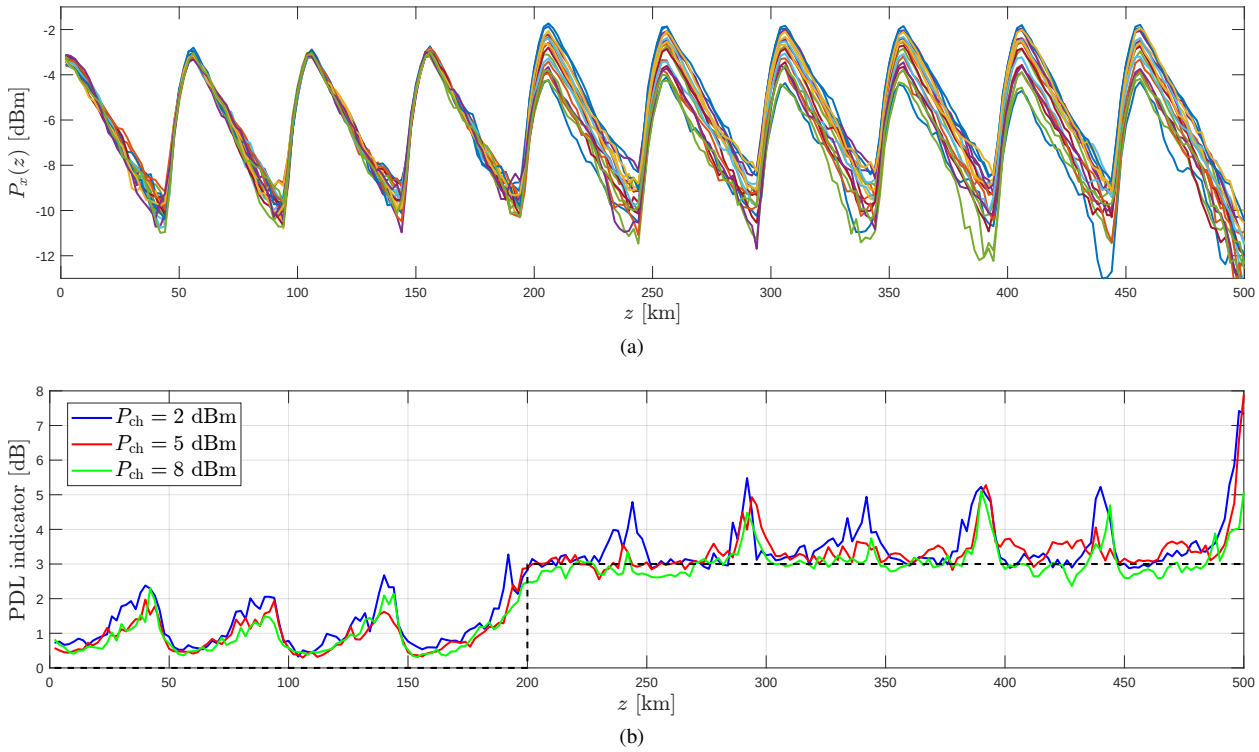

Fig. 3. (a): Power profiles, for the X-polarization, with $P_{\mathrm{ch}} = 2\,\mathrm{dBm}$. (b): PDL indicator for different transmit power with a lumped PDL element of 3 dB inserted at the beginning of the 5th span. Dashed line represents nominal value.

For each operating condition, 20 power profiles were estimated, considering a constant spatial step for the LPM algorithm of $\Delta z = 2\,\mathrm{km}$. In each profile, the SOP of the transmitted signal was randomly digitally rotated only at the transmitter, while keeping the polarization-rotation elements of the link constant. This is in line with the assumption that, in a realistic scenario, the incident state of polarization (SOP) at the PDL elements remains relatively stable over time.

Fig. 3(a) shows all the X-polarization profiles computed for a transmit power of 2 dBm. These profiles display noticeable noise, particularly in the second half of each span. The observed noise is attributed to the LPM algorithm's sensitivity to the level of nonlinearity at the measurement position; higher nonlinearity generally leads to improved accuracy in the estimation process. Thus, for such applications, it is preferable to operate at a higher power level [11]. To address this issue, a moving average operation has been performed on the estimated profiles, considering a window length of 5 samples. This post-processing step aims to mitigate the estimation noise arising from points in the link where the power is low. By averaging neighboring samples, the algorithm can partially smooth out the noise, leading to more stable and reliable estimations also at low power level, as shown by the following results. Figure 3(b) illustrates the PDL indicator for various power levels, computed as the difference between the maximum and minimum values of all profiles at each position z_k. For all powers, the PDL indicator exhibits an increase around the position $z = 200\,\mathrm{km}$, reaching approximately $3\,\mathrm{dB}$. This notable increase allows us to identify the initial part of the 5th span as the location where the lumped PDL source is situated.

To estimate the PDL value and compare the results, the mean and standard deviation of the PDL indicator are computed considering all the values between $200\,\mathrm{km}$ and $500\,\mathrm{km}$, as reported in Table I. Interestingly, the algorithm's performance at the optimal power (2 dBm) remains comparable to the performance at a higher power level (8 dBm). However, due to the limitations in accuracy mentioned earlier, the results at the optimal power exhibit more noise. This explains the appearance of peaks every $50\,\mathrm{km}$ near the end of each span. Moreover, the performance would degrade even more in an experimental scenario due to several impairments (e.g., transceiver imperfections) not present in the simulation.

TABLE I
SUMMARY OF ESTIMATION RESULTS

$\mathbf{P_{ch}}$	2 dBm	5 dBm	8 dBm
Mean PDL	3.50 dB	3.40 dB	3.07 dB
$\boldsymbol{\sigma_{\mathbf{PDL}}}$	0.77 dB	0.63 dB	0.47 dB

Fig. 4 shows the PDL indicator, computed with the same method as in Fig. 3, for different values of PDL, inserted again at the beginning of the 5th span. As expected, the accuracy of the estimation method decreases as the PDL values become smaller. Despite this, the algorithm remains capable of accurately estimating both the position and the magnitude of the PDL element, even with values as low as 1 dB.

In the presence of multiple PDL elements, the total PDL experienced by the CUT is not simply the sum of the individual PDL values, but it becomes a complex expression that depends on the alignment between the PDL axes of the single elements [16]. To test the effectiveness of the method in a distributed-PDL scenario, two lumped PDL elements were introduced in the same setup as depicted in Fig. 1. Two PDL elements,

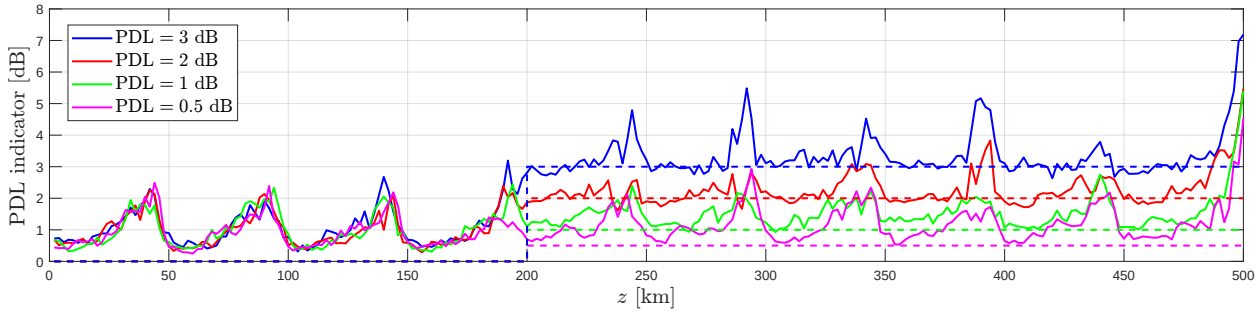

Fig. 4. PDL indicator for $P_{ch} = 2\,\mathrm{dBm}$ with different values of PDL, introduced by a lumped PDL element inserted at the beginning of the 5th span.

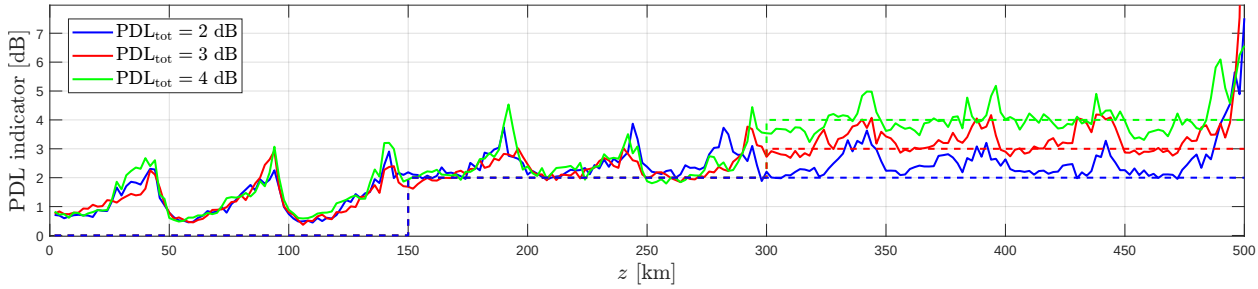

Fig. 5. PDL indicator with two lumped PDL elements in the link. A fixed 2-dB PDL element is inserted at the beginning of the 4th span, while another PDL element is inserted at the beginning of the 7th span, so that the total PDL of the link is equal to 2, 3 or 4 dB.

with a fixed value of 2 dB, were inserted at the beginning of the 4th and 7th span. By changing the relative PDL axes orientation, a different end-to-end PDL of 2, 3 or 4 dB can be obtained. Then, we ran the algorithm in each of the cases, obtaining the estimations shown in Fig. 5. In all the cases, the algorithm can accurately estimate the end-to-end PDL. The PDL indicator may then be used with threshold-based algorithms for automatic detection of lumped PDL elements.

IV. Conclusions

We proposed a novel PDL estimation algorithm in coherent optical links, based on a eRP1-LLS longitudinal power monitoring technique. In our evaluation, we tested the algorithm at power levels near the optimal range, with varying PDL values, and involving two PDL elements. The algorithm demonstrated a good accuracy across all test cases in accurately estimating both the position and the magnitude of PDL.

References

[1] T. Tanimura, S. Yoshida, K. Tajima, S. Oda, and T. Hoshida, "Fiber-longitudinal anomaly position identification over multi-span transmission link out of receiver-end signals," *J. Lightw. Technol.*, vol. 38, no. 9, pp. 2726–2733, May 2020.

[2] M. Sena *et al.*, "DSP-based link tomography for amplifier gain estimation and anomaly detection in C+L-band systems," *J. Lightw. Technol.*, vol. 40, no. 11, pp. 3395–3405, June 2022.

[3] C. Hahn, J. Chang, and Z. Jiang, "Localization of reflection induced multi-path-interference over multi-span transmission link by receiver-side digital signal processing," in *Optical Fiber Communication Conference (OFC) 2022*, S. Matsuo, D. Plant, J. S. Wey, C. Fludger, R. Ryf, and D. Simeonidou, Eds. Optica Publishing Group, 2022, p. Th1C.3.

[4] T. Sasai, E. Yamazaki, M. Nakamura, and Y. Kisaka, "Proposal of linear least squares for fiber-nonlinearity-based longitudinal power monitoring in multi-span link," in *2022 27th OptoElectronics and Communications Conference (OECC) and 2022 International Conference on Photonics in Switching and Computing (PSC)*, Toyama, Japan, 2022, pp. 1–4.

[5] A. May *et al.*, "Longitudinal power monitoring over a deployed 10,000-km link for submarine systems," in *Optical Fiber Communication Conference (OFC) 2023*. Optica Publishing Group, 2023, p. Tu2G.3.

[6] T. Sasai, M. Nakamura, E. Yamazaki, S. Yamamoto, H. Nishizawa, and Y. Kisaka, "Digital longitudinal monitoring of optical fiber communication link," *J. Lightw. Technol.*, vol. 40, no. 8, pp. 2390–2408, April 2022.

[7] M. Eto, K. Tajima, S. Yoshida, S. Oda, and T. Hoshida, "Location-resolved PDL monitoring with rx-side digital signal processing in multi-span optical transmission system," in *Optical Fiber Communication Conference (OFC) 2022*. Optica Publishing Group, 2022, p. Th1C.2.

[8] M. Takahashi, T. Sasai, E. Yamazaki, and Y. Kisaka, "DSP-based PDL estimation and localization in multi-span optical link using least squares-based longitudinal power monitoring," in *2023 Opto-Electronics and Communications Conference (OECC)*, 2023, pp. 1–6.

[9] A. D'Amico *et al.*, "Experimental probing and modeling of the PDL impact on the optical signal-to-noise ratio," in *Optical Fiber Communication Conference (OFC) 2023*. Optica Publishing Group, 2023, p. W1E.6.

[10] A. May, E. Awwad, P. Ramantanis, and P. Ciblat, "Receiver-based localization and estimation of polarization dependent loss," in *2022 27th OptoElectronics and Communications Conference (OECC) and 2022 International Conference on Photonics in Switching and Computing (PSC)*, Toyama, Japan, 2022, pp. 1–4.

[11] T. Sasai, E. Yamazaki, and Y. Kisaka, "Performance limit of fiber-longitudinal power profile estimation methods," *J. Lightw. Technol.*, vol. 41, no. 11, pp. 3278–3289, June 2023.

[12] A. Vannucci, P. Serena, and A. Bononi, "The RP method: a new tool for the iterative solution of the nonlinear schrodinger equation," *J. Lightw. Technol.*, vol. 20, no. 7, pp. 1102–1112, July 2002.

[13] P. Serena and A. Bononi, "An alternative approach to the gaussian noise model and its system implications," *J. Lightw. Technol.*, vol. 31, no. 22, pp. 3489–3499, Nov. 2013.

[14] D. Pilori, M. Cantono, A. Carena, and V. Curri, "FFSS: The fast fiber simulator software," in *2017 19th International Conference on Transparent Optical Networks (ICTON)*, Girona, Spain, 2017, pp. 1–4.

[15] S. J. Savory, "Digital filters for coherent optical receivers," *Opt. Express*, vol. 16, pp. 804–817, 2008.

[16] S. Zarkosvky and M. Shtaif, "Statistical distribution of polarization-dependent loss in systems characterized by the hinge model," *Opt. Lett.*, vol. 45, no. 5, pp. 1224–1227, Mar 2020.